OPTICAL REVIEW Vol. 18, No. 1 (2011) 60–65

Fabrication and Verification for the Small-Form-Factor Holographic Optical Pickup

Kuan Chou HOU[1], Po Chien CHOU[3], Stone CHENG[3], Yue Jheng LIN[1], Yi CHIU[1], and Jin Chern CHIOU[1,2*]

[1]*Institution of Electrical and Control Engineering, National Chiao Tung University, Taiwan 30010, R.O.C.*
[2]*School of Medicine, China Medical University, Taichung, Taiwan 40402, R.O.C.*
[3]*Department of Mechanical Engineering, National Chiao Tung University, Hsinchu, Taiwan 30010, R.O.C.*

(Received May 20, 2010; Revised October 24, 2010; Accepted October 28, 2010)

In this investigation, a small-form-factor (SFF) pickup head with a holographic optical element (HOE) is fabricated. The system employs a finite-conjugate object lens to focus a light beam. A holographic optical element is used to simplify the optical configuration. It provides a better means of alignment of fabrication and reduces the size of system relative to reflective light route. Micro prisms are fastened with HOE and a silicon substrate, laser diode and photodiode are integrated into the optical system. The pickup head system based on discrete components and a flip chip bonder with highly accurate alignment was to integrate it. The micro holographic optical pickup head is fabricated and tested. Experimental results including the spot diameter and the focusing error signal (FES), demonstrate that the optical system is a feasible.

Keywords: SFF, pickup head, Holographic optical element, HOE, virtual method

1. Introduction

In high-density optical disc systems with high numerical aperture (NA) objective lenses in optical system for small form factor optical drive, it is important to reduce the dimension of optical system. In the past few years, market for optical system such as projector, camera and pickup head grew rapidly and has enhanced the optical system unit with small form to be developed. Miniaturization of optical system has many advantages to achieve light in weight and small in size. There are many miniature way to reduce size, for example, high NA of lens[10] and reflective light route.[1,4,6,9,11] Furthermore, micro prisms with inclined process[2] and silicon-based optical element[3,8] have reliable fabrication process but these device is difficulty to apart from its own substrate to integrated with other optical devices.

A kind of small optical system was designed and simulated by Shih[5] but the study was lacked of systematic fabrication process and entire measurement results. Fabrication process of small optical was designed and implemented to demonstrate light path in expected way. In order to implement the structure and verify optical light route in the small optical system, flip chip bonder is the main technique which has high bonding precision to accomplish the focusing error signal (FES) requirement. Moreover, the holographic optical elements (HOE) have been widely applied to minimize optical system with their particular features in the functions of splitting laser beam and correcting optical aberrations. Recently study presents that HOE can be fabricated by silicon substrate with silicon nitride[3,8] which is compatible with standard semiconductor process, however, thickness of substrate is difficult to minimize size of small-form-factor (SFF) optical head.

*E-mail address: chiou@mail.nctu.edu.tw

Table 1. Specification of optical pickup head.

Item	Correspondence
Image object relation	Finite-conjugate system
Laser wavelength (nm)	635
Object NA (laser side)	0.1
Image NA (disk side)	0.65
Focal length (mm)	0.525
Clear aperture diameter (mm)	1.0
Dimensions (mm^3)	1 (H) × 3 (W) × 5 (L)

The use of HOE not only minimizes the dimension of system for a compact structure but also simplifies the light route. In this study, simulation and measurement results are successful implemented and verified.

2. Architecture of Pickup Head with Small Form Factor

This verification process describes an SFF optical system design using an HOE based on the optical specifications in Table 1. Figures 1 and 2 present the structure of the integrated pickup head, and photograph of it, respectively. The proposed devices are fabricated and tested to demonstrate their unique performances and advantages. Hence, 635 nm wavelength laser diode is expected to play an important role in stabilizing new holographic pickup structures. Figure 1, schematically depicts the pickup head including a 635 nm wavelength edge-emitting laser diode (LD), a quadrant photodetector (PD), a 45° turning mirror, two micro prisms (MP1, MP2), a HOE, a lens module, a silicon substrate with metal interconnections and a piece of printed circuit board (PCB) substrate. A 635 nm edge-emitting LD chip is the main light source in the optical system. It was bonded a silicon sub-mount with eutectic

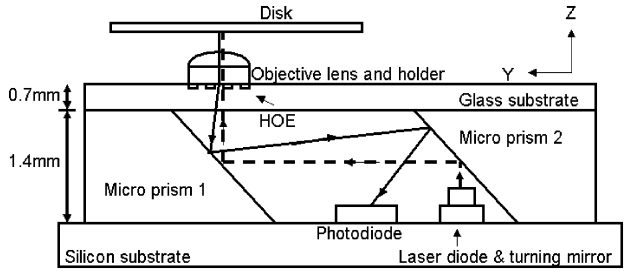

Fig. 1. Architecture of a small-form-factor holographic optical pickup.

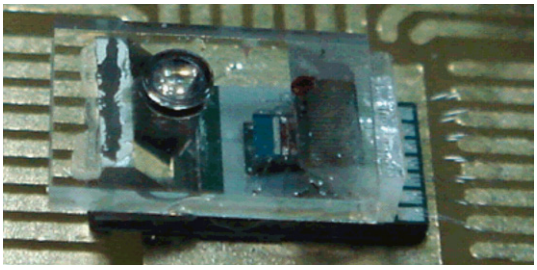

Fig. 2. (Color online) Photography of small-form-factor holographic optical pickup.

bonding to improve the thermal release efficiency and establish an interconnection, since the laser is a kind of p-side down edge-emitting LD. A PD with a quadrant PD is applied to generate FES and RF signals. The mirror and prisms work as reflective optical components to reduce the size of optical pickup head. An HOE is utilized as an optical device to produce diffraction. A lens modulus which comprised a finite-conjugate objective lens and a lens holder is to focus light beam. Figure 2 displays a photograph of the complete optical system unit. The optical layout of a laser module with the HOE is determined the astigmatic focus detection method.

3. Fabrication of Holographic Optical Element

Figure 3 and Table 2 show the structure of the fabricated HOE and measurements made of it. It serves as a beam splitter to generate the diffraction beam. An HOE was fabricated on the surface of a glass substrate that was patterned by inductively coupled plasma (ICP) etching with a depth of 352 nm. For the first order of diffraction, the measurement angle was 12% and the efficiency was 18%.

The HOE technology was presented by Shih,[5,7] it is obviously that methodology is formed as following. The HOE pattern can be designed by the binary optics technology and has the wavefront represented by

$$\phi(x,y) = \sum_{M=0}^{M}\sum_{N=0}^{N} C_{mn} X^m Y^n, \tag{1}$$

Usually, six terms is appropriate of the phase polynomial as

$$\phi(x,y) = C_{01}y + C_{20}X^2 + C_{11}xy + C_{02}y^2 + C_{21}x^2y + C_{03}y^3, \tag{2}$$

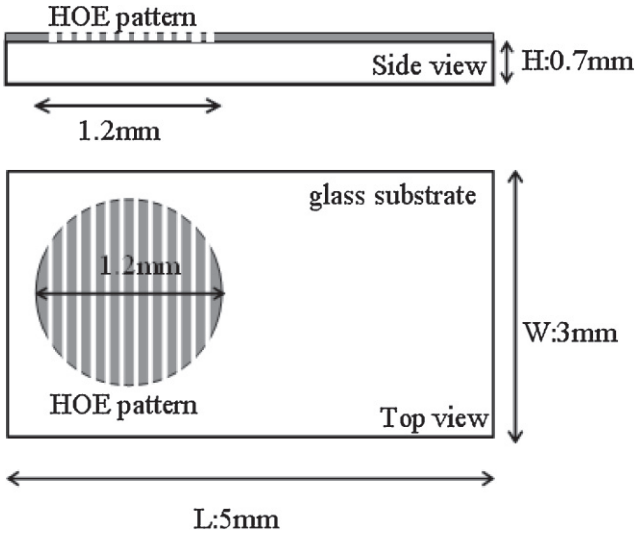

Fig. 3. Structure of holographic optical element.

Table 2. Performance of holographic optical element.

	Diffraction angles (deg)		Diffraction efficiency (%)	
	Calculated	Measured	Calculated	Measured
Zero order	0	0	40	38
First order	12.5	12	20	18

where the provides the diffraction angle in the y-direction, the $C_{20}x^2$, $C_{11}xy$, and $C_{02}y^2$ serve as the combination of a focusing lens and a cylindrical lens that converges the beam and generates the astigmatism, and the remaining terms are used for correcting the coma, spherical, and high-order aberrations. The system tolerance of the laser, PD, or micro prisms can be compensated by adjusting the HOE position. For example, shifting the HOE a distance in the negative y-axis will give the phase as

$$\begin{aligned}\phi(x, y+\Delta d) &\cong \phi(x,y) + \frac{\partial\phi(x,y)}{\partial y}\Delta d \\ &= \Delta d C_{01} + \Delta d C_{11}x + (C_{01} + 2\Delta d C_{02})y \\ &\quad + (C_{20} + \Delta d C_{21})x^2 + C_{11}xy \\ &\quad + (C_{02} + 3\Delta d C_{03})y^2 + C_{21}x^2y + C_{03}y^3, \end{aligned} \tag{3}$$

where the astigmatic term $C_{11}xy$ remains unchanged and the variation of x, y, (x^2, y^2) terms corresponds to the position change of the returning spot in the x-, y-, and z-directions, respectively.

4. Light Routing through Optical Pickup Head

Figure 4 shows the optical path of the integrated optical head, including the forward and return paths between the LD and the PD. The optical path is from the 45° turning mirror which reflects the horizontal laser beam upward to microprism 2 and redirects the light beam horizontally to microprism 1. Then, the beam is reflected upward at microprism 1 to the HOE. After the reflected beam enters the HOE

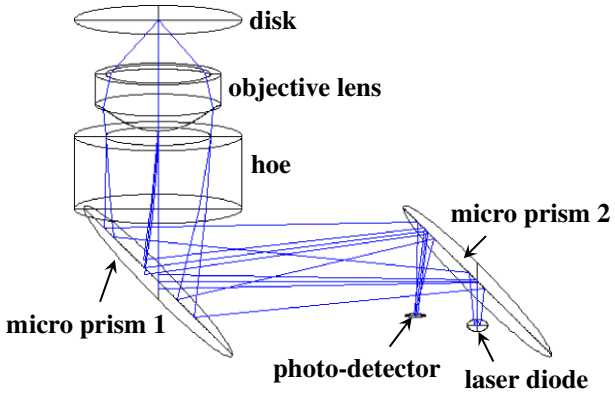

Fig. 4. (Color online) Light route of optical pickup head.

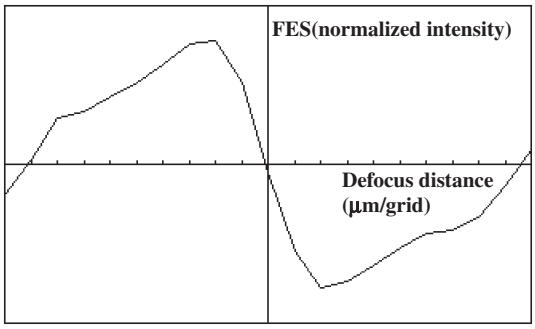

Fig. 5. Simulation result of focusing error signal.

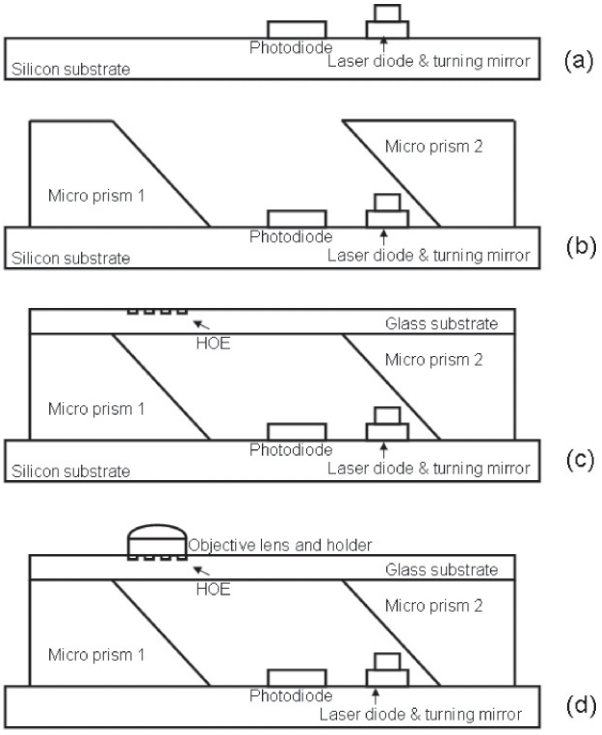

Fig. 6. Fabrication processes (a) Laser diode and photodiode. (b) Turning mirror and micro prisms. (c) HOE glass substrate. (d) Lens modulus.

perpendicularly, the zero-order laser beam passes through the objective lens and is focused on the disk. As the mentioned above, it is the forward path runs from the laser diode to the disk. The HOE is applied as a beam-splitting element to simplify the optical path and the optical components. Along the optical return path, the returning beam is diffracted by the HOE patterns, and reflected by microprism 1 horizontally to microprism 2. The micro prisms provide support to the HOE glass substrate as well as the calibration reference planes, consistent with the virtual image method. Finally, the returning beam that is projected onto the quadrant PD generates a FES, a tracking error signal (TES), and a radio frequency signal (RFS) by HOE diffraction. Figure 5 shows the simulation results of optical pickup head for a FES (S-curve).

5. LD Bonding

The process of assembling an SFF pickup head requires the precise alignment of optical pickup head to satisfy positional tolerances. Since the optical components manipulate light to the desired location, the most important operation during the assembly of the SFF pickup is the precise attachment of a temperature-sensitive laser diode. The threshold current and operating temperature crucially affect LD lifetime because increasing the operating temperature increases threshold current. Since SFF size constraints limit heat convection, heat transfer phenomena and other thermal conditions must be considered in system design. An edge-emitting LD operating at a high operating current depends on a heat sink between the active region of the device and the silicon substrate. The high thermal conductivity of a thin film of metal-dielectric enables its use in diode sub-mount applications.

The distance from the edge of the sub-mount to the LD emitting diode is a key factor in the fabrication process of diodes that are mounted with the downward bonding of their p-sides. In the high precision eutectic process, the LD emitting edge must be placed within a few microns outside the edge of the sub-mount. The laser beam is emitted at an angle from the p-side of the laser diode and the space outside the edge of the sub-mount does not reduce the brightness of the emitted laser because nothing blocks the angle of emission. Conversely, if a diode is bonded too far away from the edge of the sub-mount, then the generated heat may reduce optical performance and shut down the diode. To maximize the lifetime of the laser diode, the laser emitting orientation must be properly aligned with the edge of the sub-mount. The laser subassembly must be precisely positioned in relation to other components along the optical axis.

6. Fabrication and Calibration of Optical Pickup Head

Figure 6 displays the fabrication process of a small optical system. Firstly, a LD and a PD were bonded onto the substrate that had a patterned metal interconnection. Wire bonding was then implemented to control the driving current and acquire a signal. The turning mirror and micro prisms

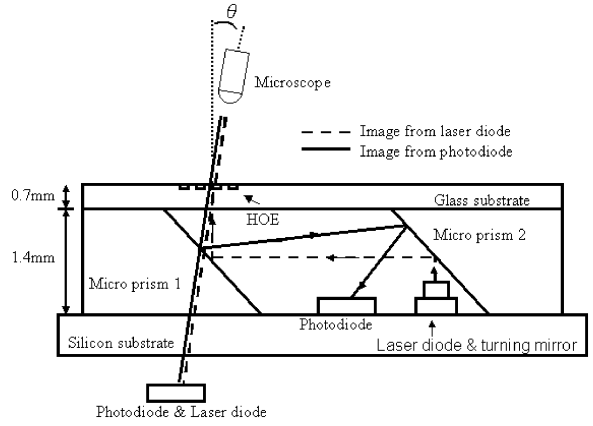

Fig. 7. Virtual image method for calibration and adjusting.

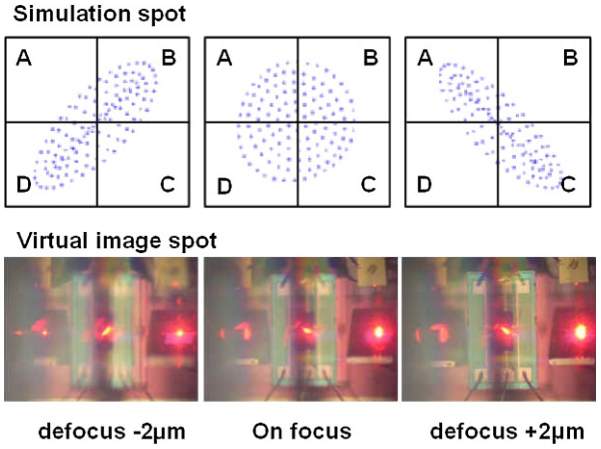

Fig. 8. (Color online) Calibration light spot of virtual image method.

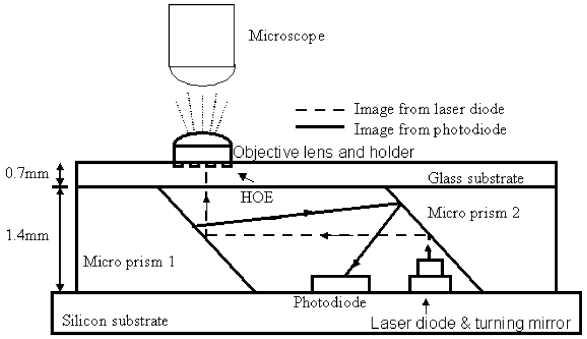

Fig. 9. Lens modulus fabrication of optical pickup head.

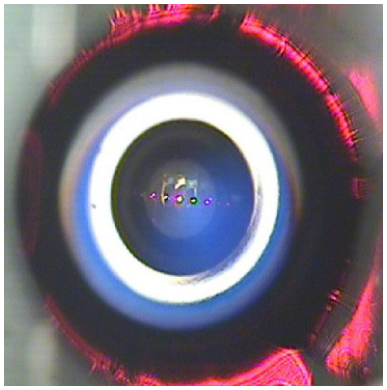

Fig. 10. (Color online) Photography of diffraction light spots on the surface of lens.

were also bonded on silicon substrate to reflect light to reduce the size of system relative to optical pickup head. A glass substrate with an HOE was bonded to both of prisms, such that the light path could be calibrated with virtual image method. The final step in fabricating the optical system was the bonding of the lens modulus to the surface of the HOE.

The virtual image method was used to calibrate an optical system with a high-precision alignment. To reflect light to the center of the quadrant photodiode, an alignment procedure can be performed to adjust the relative positions of the photodetector and the HOE, as in Fig. 7. The virtual image of the laser is obtained by extending the diffracted beam to the virtual focal image, which must coincide with the location of the photodetector image. Since the HOE and the other integrated unit were aligned with virtual image method in the established light path, optical alignment was conducted by replacing microprism 1 and the HOE glass to calibrate the lateral and circular displacement of system layout in a specific fixture apparatus with a tilted angle. The fixture apparatus is applied to setup experiment of virtual image method and the optical pickup head is fastened on it to calibrate its tolerance. Therefore, alignment tolerances among the LD, turning mirror, and micro prisms assembly are eliminated and the precision of light path that begins at LD and is reflected to the center of PD is ensured in the small optical system.

Figure 8 presents virtual images of calibration obtained with various focal points. The light spot is focused and defocused on the center of the quadrant detector repeatedly. The method of calibrating is astigmatic returning method and the simulated spots are presented for comparison with actual measured result.

After the microprisms and the HOE were attached to the optical module, the objective lens unit was the final component to be assembled. A mechanical *xyz* stage was utilized to assemble the objective lens unit on the optical module to minimize aberrations such as coma, astigmatism, and spherical aberration. Figure 9 shows the architecture of bonded lens. It utilizes the HOE with characteristic of diffraction to produce five light spots on the surface of the lens which are observed under a microscope. These light spots exhibit the diffraction phenomena that are shown in Fig. 10. Finally, an ultraviolet curable epoxy was used to attach the integrated subassembly to the objective lens module. This step is very important for lens modulus fabrication because it ensures the success of the bonding process. However, the phenomena do not indicate that the fabrication was successful due to the main technique for calibration is virtual method.

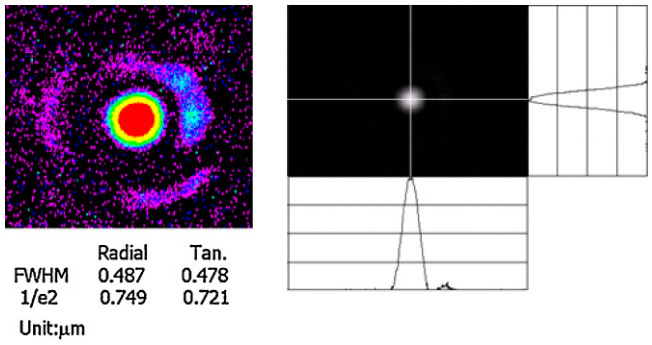

Fig. 11. (Color online) Measurement result of focused light spot.

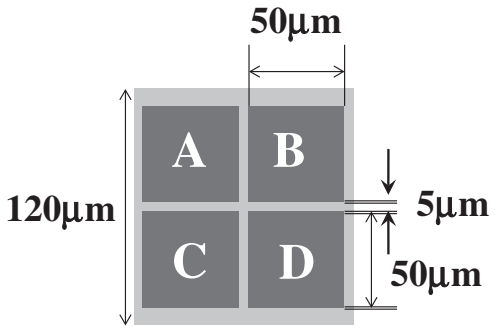

Fig. 12. Dimension of photodiode.

Table 3. Specification of photodiode.

Specification	Value
Breakdown voltage (V)	>10
Sensitivity (A/W)	>0.4 (635 nm)
Dark current (nA)	2
Crosstalk (%)	15 (gap 5 μm)
Rise and fall times (ns)	<5

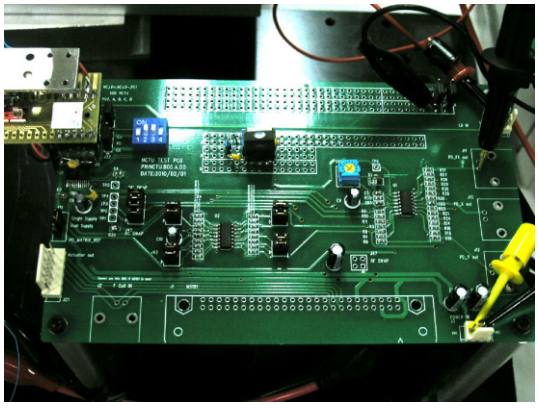

Fig. 13. (Color online) A signal conversion circuit of photodiode.

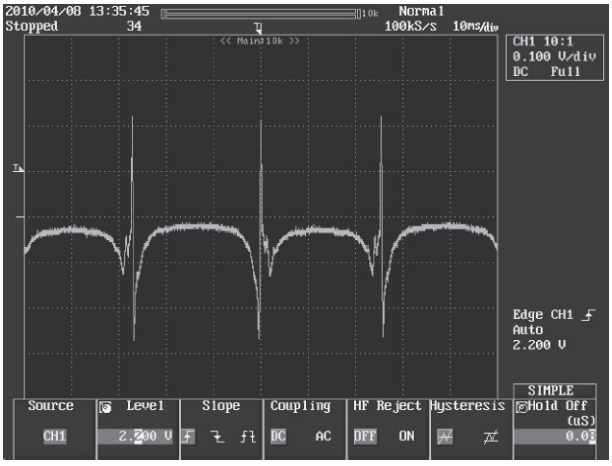

Fig. 14. Measurement of focusing error signal (S-curve).

7. Experimental Results

Figure 11 plots the measurements of the size of the focusing spot which includes radial and tangential spot distributions. Although the full-width at half-maximum (FWHM) spot size in the radial direction of the disc exceeded that in the tangential direction, the spot intensity of the spot was normally distributed.

The experimental setup for analyzing the performance of the integrated SFF optical device included an integrated SFF pickup unit, an actuator, an optical signal conversion amplifier, and a mini disc medium. The quadrant detector exploited the astigmatic method for focusing and the push–pull method for tracking. The actuator is a four wire voice coil motor (VCM) actuator. It uses the voice coil motor to be the main component of the actuator. Table 3 shows the specifications of photodetector. Figure 12 also shows layout of four segmented cells for extracting the FES and RF (A, B, C, and D). The length of each segmented is 50 μm and the space between the detection areas is 5 μm.

Figure 13 displays the experimental setup for FES measurement. A signal conversion circuit was implemented and tested with PCB. Figure 14 presents the FES that was obtained by the astigmatic focusing method. The horizontal axis represents defocus position, and the vertical axis represents optical signal. The output signal is calculated as $(A + C) - (B + D)$, and detected by the quadrant detectors. To verify the focusing performance of this HOE optical module, the focusing actuator was driven by a 5 Hz triangular signal with amplitude of ±140 mV to bring the optical module past its focal point to the disc. A comparison of the simulated results and dynamic experimental data reveals that the measured results were satisfactory and demonstrated the feasibility of the SFF pickup head.

8. Conclusions

This investigation proposes a new optical pickup head with small form factor, with a demonstrably feasible fabrication process. The small optical system has height, width and length of $1 \times 3 \times 5\,\text{mm}^3$. The pickup head system using existing discrete components was demonstrated, and a flip chip bonder with highly accurate alignment was to integrate it. The SFF pickup with the HOE was fabricated to

meet optical specifications to simplify the optical architecture and minimize the scale of the device. To ensure that the optical system performs reliably, the temperature-sensitive laser diode must be accurately assembled with a silicon submount with a high capacity for thermal release to ensure its alignment. After the reference optical path was established, the virtual image method with HOE pattern alignment was performed to achieve an optical configuration. Finally, the experimental results of the spot diameter, FES, and the efficiency of light path through prisms and holographic elements are demonstrated. This integrated SFF pickup head with HOE is a feasible for use in next-generation optical storage systems.

Acknowledgments

This work was supported in part by Ministry of Economic Affairs, Taiwan, R.O.C. under contract No. 97-EC-17-A-07-S1-011, and the National Science Council, Taiwan, R.O.C. under contract no. NSC-98-2220-E-009-014, NSC-98-2220-E-009-032, and NSC-98-2218-E-039-001. It was also supported in part by Taiwan Department of Health Clinical Trial and Research Center of Excellence under contract No. DOH99-TD-B-111-004 and No. DOH99-TD-C-111-005.

References

1) Y. Komma, S. Kadowaki, S. Nishino, Y. Hori, and M. Kato: Opt. Rev. **3** (1996) 251.
2) F. G. Tseng and H. T. Hu: Proc. 12th Int. Conf. Solid State Sensors, Actuators and Microsystems, 2003, p. 599.
3) Y. C. Chang, C. M. Wang, and J. Y. Chang: Opt. Express **28** (2003) 1260.
4) J.-S. Sohn, S.-H. Lee, M.-S. Jung, T.-S. Song, N.-C. Park, and Y.-P. Park: Microsyst. Technol. **11** (2005) 457.
5) H.-F. Shih, C.-L. Chang, K.-J. Lee, and C.-S. Chang: IEEE Trans. Magn. **41** (2005) 1058.
6) K.-S. Jung, H.-M. Kim, S.-J. Lee, N.-C. Park, S.-I. Kang, and Y.-P. Park: Microsyst. Technol. **11** (2005) 1041.
7) H.-F. Shih: Jpn. J. Appl. Phys. **44** (2005) 1797.
8) J.-Y. Chang, C.-M. Wang, C.-C. Lee, H.-F. Shih, and M.-L. Wu: IEEE Photonics Technol. Lett. **17** (2005) 214.
9) S.-M. Kang, J.-E. Lee, W.-C. Kim, N.-C. Park, Y.-P. Park, E.-H. Cho, J.-S. Sohn, and S.-D. Suh: Jpn. J. Appl. Phys. **45** (2006) 6723.
10) D. L. Blankenbeckler, B. W. Bell, Jr., K. Ramadurai, and R. L. Mahajan: Jpn. J. Appl. Phys. **45** (2006) 1181.
11) Y. Chiu, H.-F. Shih, J.-C. Chiou, S.-T. Cheng, K.-Y. Hung, F.-G. Tseng, and W. Fang: IEEE Trans. Magn. **45** (2009) 2194.